Parameterization of an Electrical Battery Model for Dynamic System Simulation in Electric Vehicles

Markus Einhorn*, Valerio F. Conte*, Christian Kral*, Jürgen Fleig** Robert Permann*

* AIT Austrian Institute of Technology,
Mobility Department, Electric Drive Technologies,
Giefinggasse 2, 1210 Vienna, Austria
markus.einhorn@ait.ac.at
** Vienna University of Technology
Institute of Chemical Technologies and Analytics,
Getreidemarkt 9/164EC, 1060 Vienna, Austria

***Abstract*—This article describes the parameterization of a simple, dynamic single cell battery model for cell and system simulation. It is shown how to parameterize the model based on basic electrical tests and publicly available data such as data sheets. The performance of the parameterized model is validated with test results gained from two different cycles with the li-Tec HEA 40 High Energy Cell. Additionally, it is shown how the model can be extended to consider basic aging effects.**

***Index Terms*—Lithium-ion battery, battery model, impedance, parameter extraction, aging.**

I. Introduction

Applications of batteries are increasing rapidly in every part of life and it is only a matter of time until the number of hybrid electric vehicles (HEV), cars with range extenders or even pure electric cars exceed the number of cars with conventional power train. The more applications arise the greater is the need for powerful batteries which leads directly to the lithium ion technology [1].

Prototyping, by using the results from previous simulation, is a common used technique to reduce time consuming tests because some of these tests can be simulated if an accurate model exists. It is usually much cheaper to perform virtual tests since no expensive test and measurement equipment is required and parallel use of the same simulation-model at the same time on different workstations is possible.

Many battery models with various focus and applications have already been proposed [2], but the implementation and the parameterization is mostly complicated and time consuming. Therefore, this article is focused on an electrical battery model with good tradeoff between performance, complexity and parameterization work [3]. The model is explained in detail and moreover, it is shown how to parameterize it with data gained from basic electrical tests and publicly available data. The parameterized model is compared with test results gained from a real life cycle and a standard discharging procedure with the li-Tec HEA 40 High Energy Cell [4]. Finally, the main aging effects can be taken into account in an extended version of the model to assure the accuracy of the model for long term application.

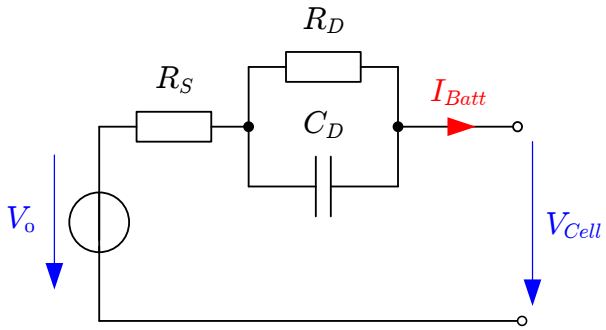

Fig. 1. Basic electrical battery model.

II. Battery Model

A commonly used electrical battery model is shown in figure 1 [3], [5]. This model avoids solving a system of coupled, time-varying partial differential equations which occur typically in electrochemical models [6]. It has more direct relation between the model parameters and the battery behavior than pure mathematical models, which do not need any system knowledge (black box approach) [7]. Therefore it offers a good tradeoff between performance, complexity and usability.

The components of the model are

- V_0 the voltage source, which characterizes the open circuit voltage (OCV),
- R_S the ohmic impedance of the contacts, the electrodes as well as the electrolyte and
- R_D, C_D which characterize the transient response of the battery electrodes.

Figure 2 exemplarily shows the ideal Nyquist plot of the internal impedance for this basic battery model. The same information is contained in the step response of a current step applied to the internal impedance. Figure 3 shows a current step of $40\,\mathrm{A}$ and the calculated step response of the internal impedance [8]. The most difficult task for implementation is getting the correct parameters for the model specially when some components are varying during simulation. Therefore an

978-1-4244-8218-4/10/$26.00 ©2010 IEEE

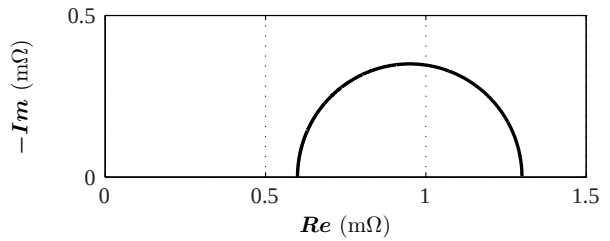

Fig. 2. Ideal Nyquist plot of the internal impedance of the basic battery model with $R_S = 0.6\,\mathrm{m\Omega}$, $R_D = 0.7\,\mathrm{m\Omega}$ and $C_D = 70000\,\mathrm{F}$.

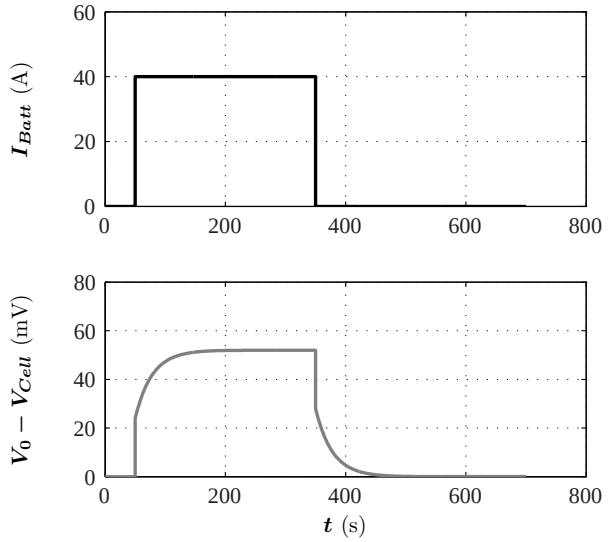

Fig. 3. Voltage response when a rectangular current pulse of $I_{step} = 40\,\mathrm{A}$ is applied to the battery impedance of the basic battery model with $R_S = 0.6\,\mathrm{m\Omega}$, $R_D = 0.7\,\mathrm{m\Omega}$ and $C_D = 70000\,\mathrm{F}$.

initial start value and a second parameter which considers the change have to be defined. Some components are changing during one cycle as well as during the whole lifetime of a cell as described in section VI.

III. Modeling

The simulation language used for this approach is Modelica/Dymola because of the simple and object-oriented possibility to model interdisciplinary relations [9].

A. Parameters and output variables

The input parameters for the basic model are

C_N	the rated capacity in Ah,
$CycleNr_0$	the initial number of cycles,
SOC_X, OCV_X	pointwise approximation of the OCV in V versus the SOC,
SOC_0	the initial state of charge,
R_{S0}	the ohmic resistance of the electrolyte and the contacts in Ω at $SOC = 0$,
$k_{R_S SOC}$	the coefficient for the change of R_S over SOC in Ω,
R_{D0}	the ohmic resistance of the electrodes in Ω at $SOC = 0$,
$k_{R_D SOC}$	the coefficient for the change of R_D over SOC in Ω,
C_{D0}	the capacitance of the electrodes in F at $SOC = 0$ and
$k_{C_D SOC}$	the coefficient for the change of C_D over SOC in F.

Given a current I_{Batt} over time the following variables are calculated:

SOC	the state of charge of the cell,
$CycleNr$	the number of cycles,
R_S	the ohmic resistance of the electrolyte and the contacts Ω,
R_D	the ohmic resistance of the electrodes in Ω,
C_D	the capacitance of the electrodes in F,
V_0	the (theoretical) OCV in V and
V_{Cell}	the cell voltage in V.

Dependencies on temperature, current amplitude and current shape are neglected in this model.

B. Estimation of the output variables

The state of charge

$$SOC = \frac{C_N - Q}{C_N}, \tag{1}$$

with the already removed charge at time instant t_0

$$Q = \int_0^{t_0} I_{Batt}(t)dt, \tag{2}$$

is a value between zero and one and describes the available charge based on the rated capacity C_N. The actual rated capacity C_N is the available charge in a fully charged cell.

One cycle is defined as the double rated capacity charge transfer to or from the cell (Coulomb counter). This can be discharging, starting from any SOC_α until discharge voltage limit DVL, charging until charging voltage limit CVL and discharging again until SOC_α. Equivalent treated is charging, starting from SOC_β to CVL, discharging until DVL and charging until SOC_β. Therefore

$$CycleNr = CycleNr_0 + \frac{1}{2 \cdot C_N} \cdot \int_0^{t_0} |I_{Batt}(t)|\,dt \tag{3}$$

is defined since also part-cycles have to be considered.

The OCV is a function of the SOC and although it could be defined by a polynomial

$$U_0(SOC) = a_0 + a_1 \cdot SOC + \ldots + a_n \cdot SOC^n, \tag{4}$$

experience showed that the result is not satisfying with $n = 3$ and polynomials tend to oscillate with higher grade [10]. A better approach would make use splines but the best result has been gained (regarding error and effort) with a linear interpolation between several supporting points, which are also very easy to measure. Figure 4 shows the measured supporting points and the interpolation for the li-Tech HEA40 cell [4] .

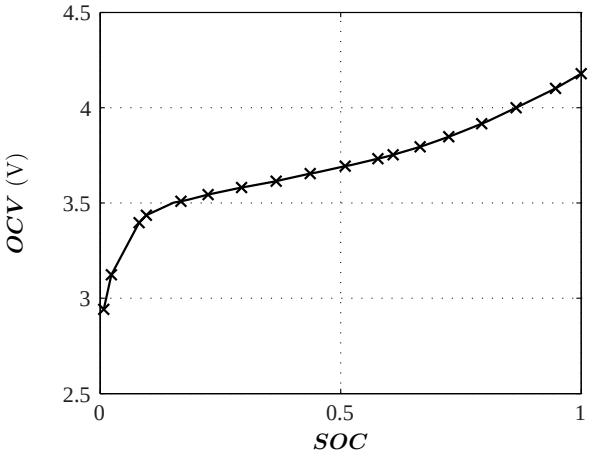

Fig. 4. Linear interpolation of the OCV for different SOC gained from Hybrid Pulse Power Characterization tests for the li-Tech HEA40 cell [11], [4].

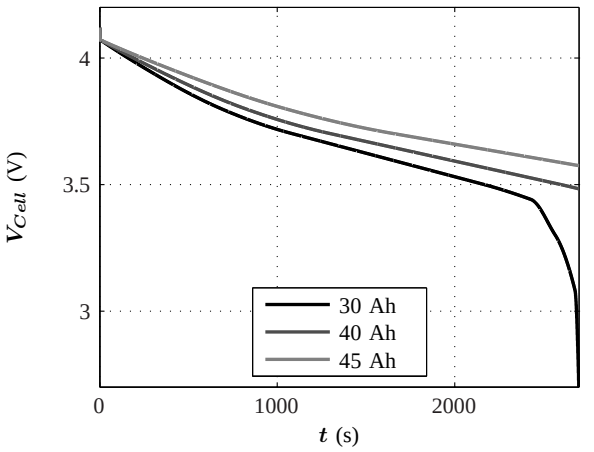

Fig. 5. Simulation of the cell voltages of 3 serial connected cells with capacities between 30 Ah and 45 Ah when applying a 40 A constant discharging current.

When serially connected cells with different C_N are stressed with the same discharging current, their voltage shape appears different even if the OCV shape is the same (5).

The internal impedance varies with different SOC as shown in figure 6 for the cell used in this study. Although the measured impedance behavior from the cell (figure 6) is not completely the same as from the model (figure 2), only R_S, R_D and C_D are considered in the model. R_S can be implemented as

$$R_S(SOC) = R_{S0} + k_{R_S SOC} \cdot SOC. \tag{5}$$

R_D and C_D) can be modeled in the same manner if necessary.

The model would not get much more complicated if the linear interpolation for $R_S(SOC)$, $R_D(SOC)$ and $C_D(SOC)$ (if implemented) is replaced with polynomials or lookup tables but the accuracy would be improved only slightly and the amount of parameters then increases a lot. If in the present implementation, a parameter (k_x) is not available, its effect

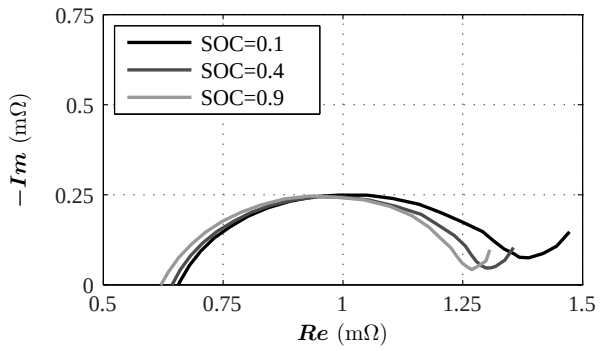

Fig. 6. Nyquist plot of the internal impedance for different SOC of the li-Tech HEA 40 measured with a current of 0.6 A between 0.1 and 400 Hz.

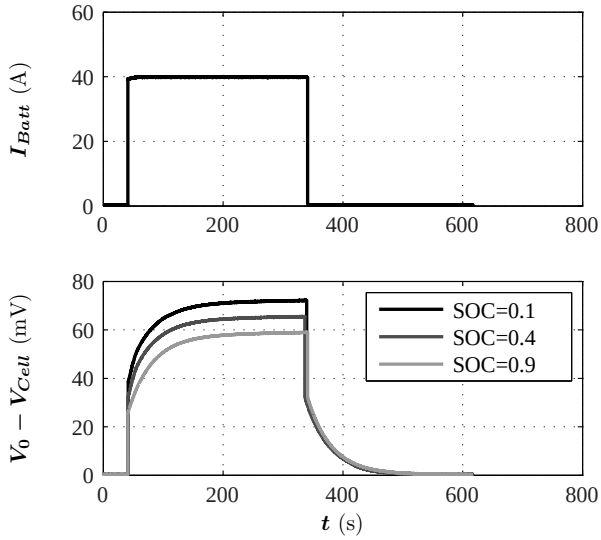

Fig. 7. Measured voltage response of the internal impedance for different SOC of the li-Tech HEA 40 when applying a current step of 40 A.

could be disabled by setting the responsible k_x value to zero.

IV. Parametrization

The rated capacity C_N can be deduced from the data sheet of the battery manufacturer or measured [4]. The shape of the OCV versus SOC curve can either be extracted from data sheet or measured. The initial number of cycles $CycleNr_0$ as well as the initial State of Charge SOC_0 are experiment specific parameters while the determination of the others will be described in the following.

The impedance parameters can be obtained by performing an electrical impedance spectroscopy measurement as described in literature [12]. If no impedance spectrometer is available the parameters can also be found by applying a current pulse and measuring the voltage response as shown in figure 3 and 7 (assuming linearity of the system). With I_{step}, the step height of the current and the initial voltage response V_{step} the serial ohmic resistance can be estimated

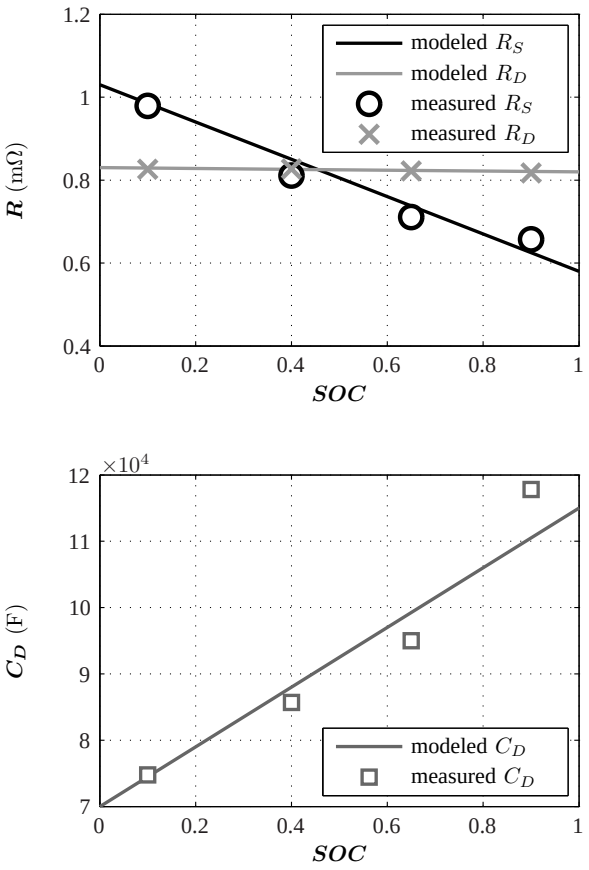

Fig. 8. Supposed alteration of R_S, R_D and C_D over SOC. The impedances were extracted from voltage step responce with a step current of 40 A.

for a specific SOC with

$$R_S = \frac{V_{step}}{I_{step}}. \tag{6}$$

While R_D can be found from

$$R_D = \frac{V_{final}}{I_{step}} - R_S, \tag{7}$$

rearranging the equation for the time constant of the exponential curve delivers

$$C_D = \tau \cdot \frac{R_S + R_D}{R_S \cdot R_D}. \tag{8}$$

Figure 8 shows the resistive and capacitive data deduced from current pulse experiments on the li-Tec HEA40 battery (figure 7) and the implemented curves for R_S, R_D and C_D.

A battery is a nonlinear device and the measurement current rate influences the result. This is the reason why the parameters in figure 8 are slightly different from those deduced from impedance spectrometer measurement (figure 6).

V. Validation

For a realistic validation of the parameterized model, the current profile gained from the FTP72 cycle is applied to the model as well as to the real cell (li-Tech HEA40). The FTP72

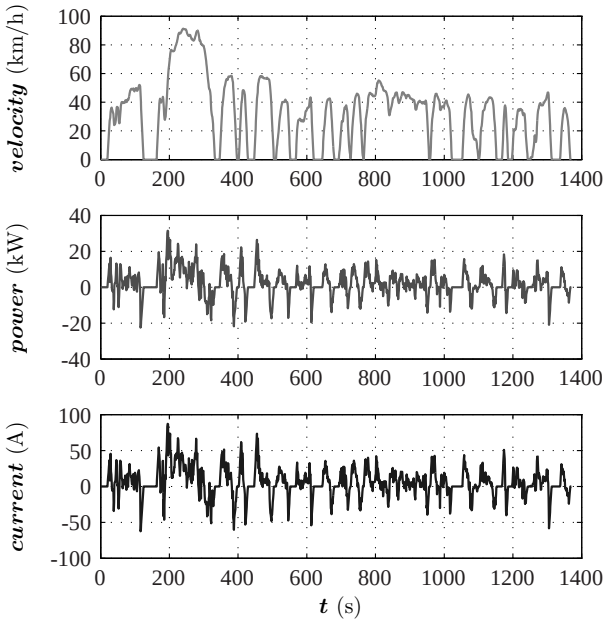

Fig. 11. Definition of the FTP72 driving cycle, power consumption of a typical electrical vehicle and current requirement from a battery pack with 100 serial connected single cells with a cell voltage of 3.6 V respectively.

cycle, defined in [13], is a standardized real life cycle and simulates an urban route of 12.07 km. This cycle was applied to a compact electric vehicle to extract a realistic power and current profile. The power and current profile are shown in figure 11. The current profile is repeated starting from the full charged cell until discharging voltage limit DVL is reached. Figure 9 and 12 shows that the error, related to the measured voltage, between the simulated and the measured voltage stays below 0.5% for $SOC = [1, 0.1]$ and below 1.5% during the entire discharging process. The same approach is performed with a less dynamic cycle [11] to show the properness of the model (figure 10 and 13). During the whole test the cell was in a climate chamber with an ambient temperature of 40°C to minimize temperature effects (figure 14).

All results thus demonstrate, that the model, parameterized with measurements or values from data sheets, is able to reproduce sophisticated real life cycles.

VI. Inclusion of aging effects in future work

A. Aging effects

Research on aging aspects of Li-ion battery behavior is still in an early stage. Tests are very time and cost consuming and many parameters influence the results in a complex manner. Although the main aging mechanisms are well known [14], it is hardly possible to model all the relevant process especially when a system-oriented simulation is preferred.

Basically, there is a difference between calendar aging and aging due to cycling. Li-ion cells typically have a calendar lifetime of approximately 2 to 4 years. In this time the internal impedance increases and the rated capacity C_N decreases [15]. The end of life (EOL) is defined to be reached when the rated

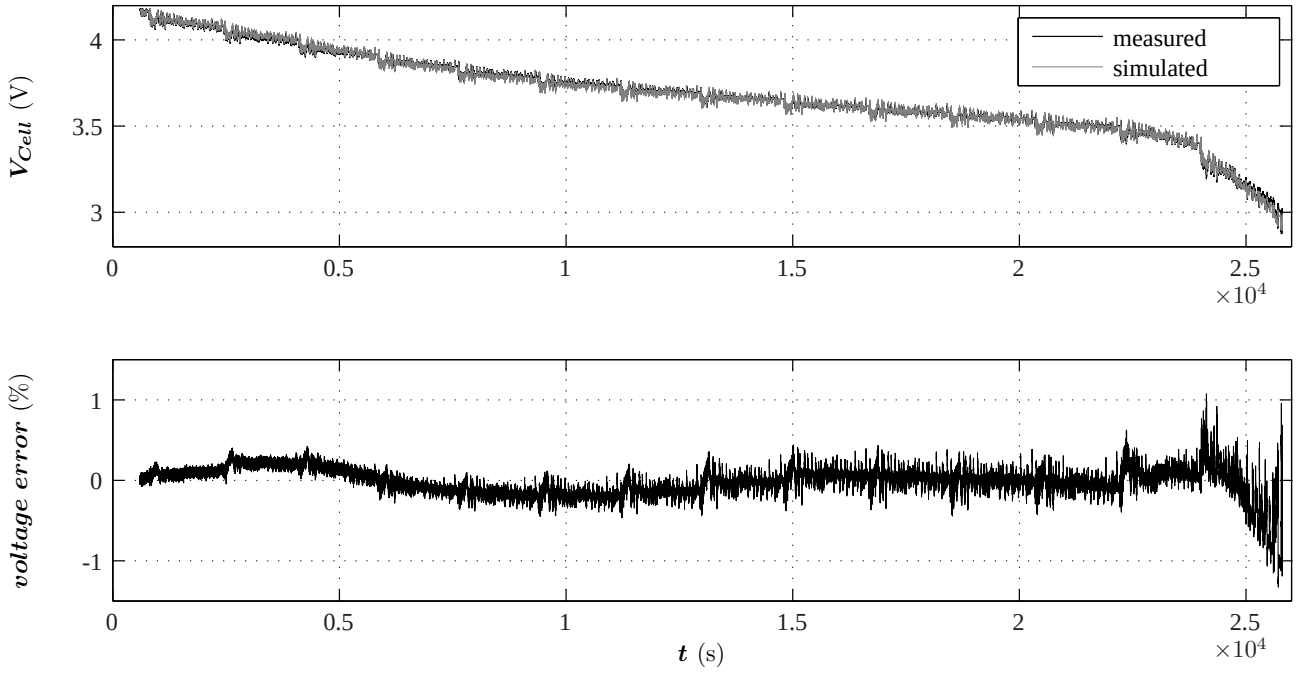

Fig. 9. Comparison of the measured and simulated cell voltage when applying the FTP72 current profile from figure 11 continuously repeated (top). The error refers to the measured voltage (bottom).

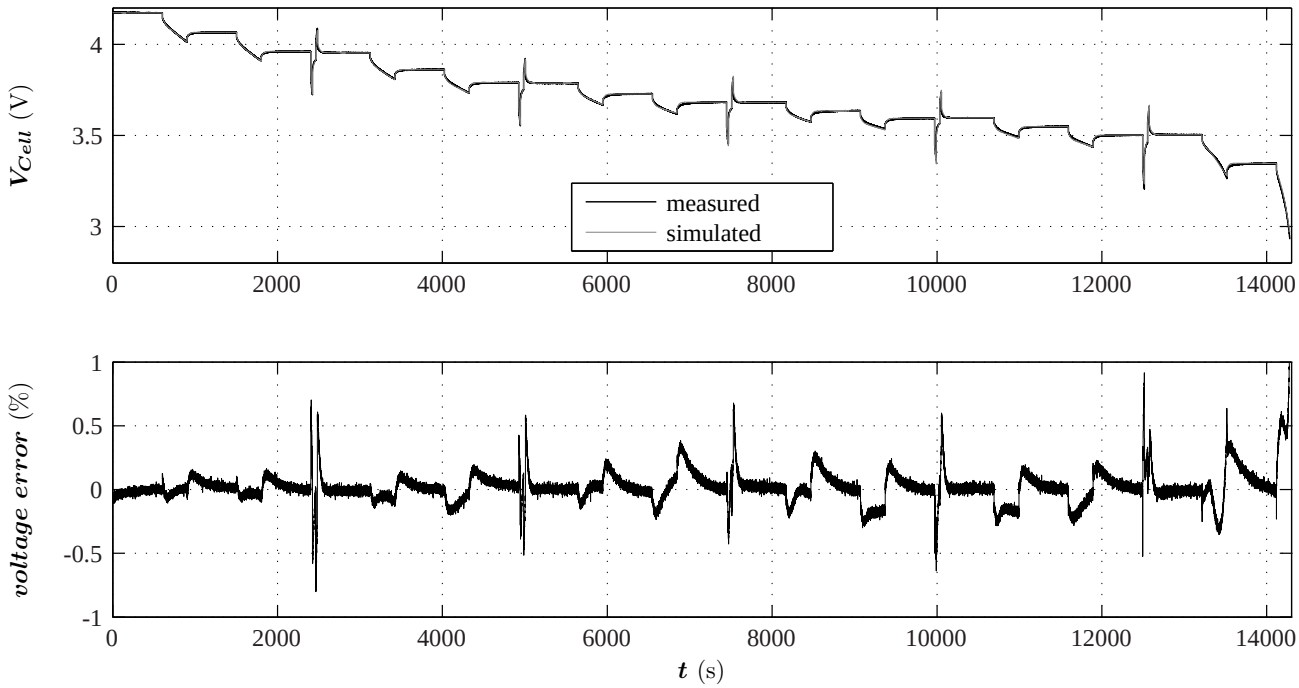

Fig. 10. Comparison of the measured and simulated cell voltage when applying a current profile as defined in the HPPC test procedure (top) [11]. The error refers to the measured voltage (bottom).

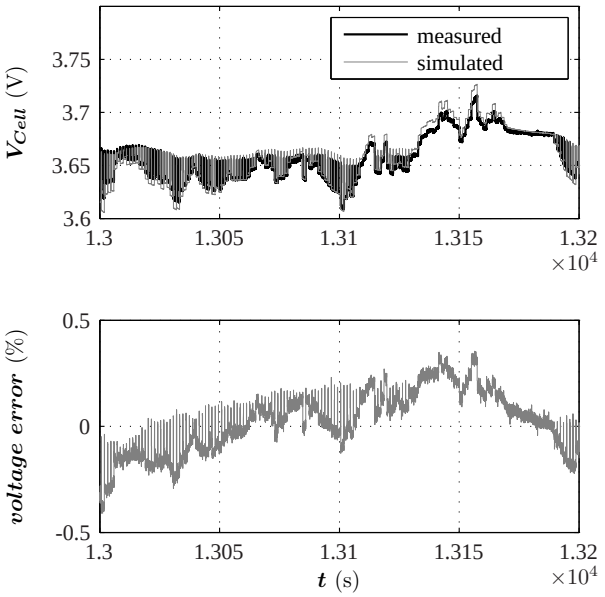

Fig. 12. Detail of the comparison from figure 9 at $SOC \approx 0.5$.

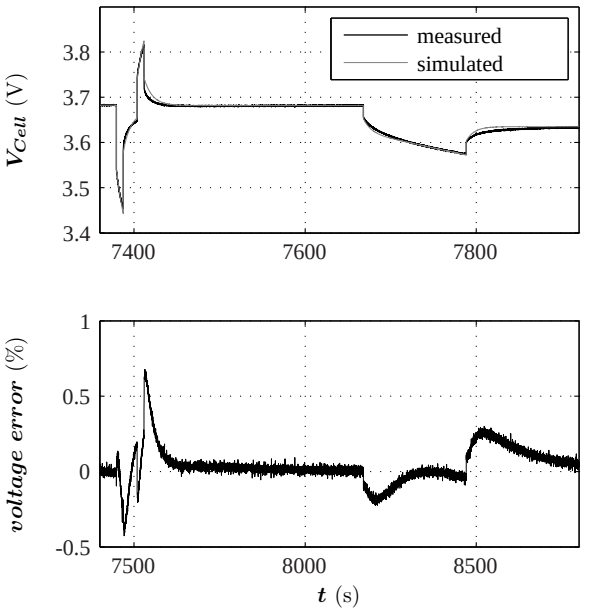

Fig. 13. Detail of the comparison from figure 10 at $SOC \approx 0.5$.

capacity is reduced by $20\,\%$ from the initial value. Furthermore, the rated capacity is not only altered with increasing cycle number but is also influenced by some other factors (discharging current, temperature, cycle shape, etc.).

The ohmic impedance mainly increases due to changes of the electrolyte (e.g. electrolyte consumption), the electrolyte/electrode interface and changes of the contact resistance [16].

Fig. 14. Climate chamber to guarantee a constant temperature of 40°C during cycling.

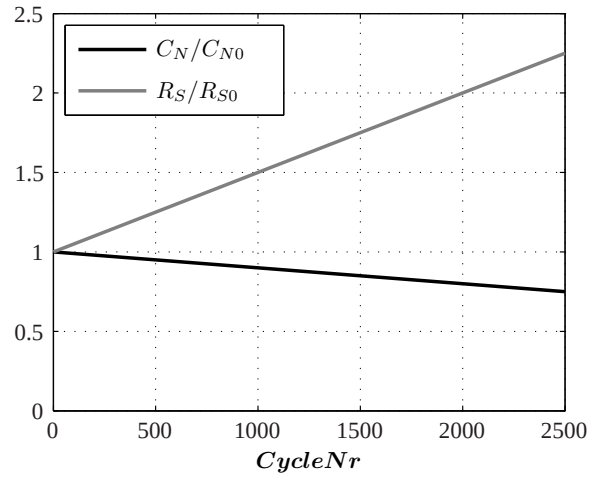

Fig. 15. Supposed alteration of the rated capacity C_N and the internal resistance R_S due to cell cycling [17].

B. Extension of the model

In the extended model, a linear reduction of the capacity C_N and a linear growth of the internal resistance R_S over the number of cycles $CycleNr$ can be taken into account as shown in figure 15 [17].

The additional input parameters for the model are

C_{N0}	the initial rated capacity in Ah,
k_{C_N}	the aging coefficient of the rated capacity in $\mathrm{Ah}/CycleNr$,
R_{S0}	the initial ohmic resistance of the electrolyte and the contacts in Ω at $SOC = 0$,
$k_{R_S CycleNr}$	the aging coefficient for R_S over $CycleNr$ in Ω.

The additional output variables are

C_N the actual capacity of the cell in Ah,
R_S the actual ohmic resistance of the electrolyte and the contacts Ω,

The rated capacity C_N decreases from C_{N0} depending on the cycle number $CycleNr$ due to aging by means of

$$C_N(CycleNr) = k_{C_N} \cdot CycleNr + C_{N0} \tag{9}$$

The parameter k_{C_N} can usually be extracted from data sheet. Taking aging due to cycling into account, (5) can be extended to

$$R_S(CycleNr, SOC) = R_{S0} + k_{R_S CycleNr} \cdot CycleNr + k_{R_S SOC} \cdot SOC. \tag{10}$$

VII. Conclusion

A cell model for dynamic cell and system simulation including the parameterization has been presented. The model can be easily parameterized using data sheet and impedance spectroscopy or applying a current impulse to the contacts while measuring the voltage response. The model has been parameterized for a specific battery (li-Tec HEA40) and validated using two different, standardized cycles. The error between measured and simulated voltage stays below $1.5\,\%$ during the whole discharging cycle and emphasises the accuracy of the model. The model has been extended in order to consider basic aging effects.

Further work will focus on how the measuring current influences the internal impedance for both presented parameter extraction methods (voltage step response and electrical impedance spectroscopy) and will cover a validation of the extended model with aging data, when available. Next versions of the model will also include temperature behaviour.

Acknowledgments

The authors would like to acknowledge the help by Johannes Starzinger from MAGNA STEYR for providing the electrical impedance spectrometer measurements and the measurement of the FTP72 driving cycle.

References

[1] C. Rosenkranz, C. Kupfer, and U. Köhler, "Battery challenges," *21th International AVL Conference Engine and Environment*, September 2009.
[2] D. S. H. L. Chan, "A new battery model for use with battery energy storage systems and electric vehicles power systems," *IEEE Power Engineering Society Winter Meeting*, 2000.
[3] *FreedomCAR Battery Test Manual For Power-Assist Hybrid Electric Vehicles*, U.S. Department of Energy, 2003.
[4] *HEA 40 High Energy Cell Datasheet*, Li-Tec, 2008.
[5] L. Gao, S. Liu, and R. A. Dougal, "Dynamic lithium-ion battery model for system simulation," *IEEE Transaction on Components and packaging technologies*, vol. 25, Nr. 3, 2002.
[6] J. Newman, K. E. Thomas, H. Hafezi, and D. R. Wheeler, "Modeling of lithium-ion batteries," *Journal of Power Sources*, vol. 119-121, pp. 838 – 843, 2003.
[7] R. C. Kroeze and P. T. Krein, "Electric battery model for use in dynamic vehicle simulations," *IEEE Power Electronics Specialists Conference*, 2008.
[8] S. Lee, J. Lee, and B. H. Cho, "State-of-charge and capacity estimation of lithium-ion battery using a new open-circuit voltage versus state-of-charge," *Journal of Power Sources*, vol. 185, 2008.
[9] P. Fritzson, *Principles of Object-Oriented Modeling and Simulation with Modelica 2.1*. IEEE Press, Wiley-Interscience, 2004.
[10] I. N. Bronstein and K. A. Semendjajew, *Taschenbuch der Mathematik*. Harri Deutsch, 2008.
[11] *USABC Battery Test Procedures Manual*, USABC, DOE National Laboratories, 1996.
[12] *Application Note - Basics of Electrochemical Impedance Spectroscopy*, Gamry Instruments, 2007.
[13] *FTP72 Urban Dynamometer Driving Schedule (UDDS)*, U.S. Environmental Protection Agency.
[14] J. Vetter, P. Novak, M. R. Wagner, C. Veit, K.-C. Möller, J. Besenhard, M. Winter, M. Wohlfahrt-Mehrens, C. Vogler, and A. Hammouche, "Ageing mechanisms in lithium-ion batteries," *Journal of Power Sources*, vol. 147, 2005.
[15] U. Tröltzsch, O. Kanoun, and H.-R. Tränkler, "Characterizing aging effects of lithium ion batteries by impedance spectroskopy," *Electrochimica Acta*, September 2005.
[16] A. Jossen and W. Weydanz, *Moderne Akkumulatoren richtig einsetzen*, 1st ed. Reichhardt Verlag, 2006.
[17] M. Broussely, P. Biensasn, F. Bonhomme, P. Blanchard, S. Herreyre, K. Nechev, and R. J. Staniewicz, "Main aging mechanisms in li ion batteries," *Journal of Power Sources*, vol. 146, May 2005.